

Experimental investigation on heat transfer rate of Co–Mn ferrofluids in external magnetic field

M. MARGABANDHU^{1*}, S. SENDHILNATHAN², S. SENTHILKUMAR³, K. HIRTHNA⁴

¹Anna University Chennai: University College of Engineering-Ariyalur, Department of Physics, Ariyalur-621704, India

²Anna University Chennai: University College of Engineering-Pattukkottai, Department of Physics, Rajamadam-614701, Thanjavur, India

³Anna University Chennai: University College of Engineering-Ariyalur, Department of EEE, Ariyalur-621704, India

⁴Anna University Chennai: University College of Engineering-Kanchipuram, Department of Physics, Kanchipuram-631552, India

Manganese substituted cobalt ferrite ($\text{Co}_{1-x}\text{Mn}_x\text{Fe}_2\text{O}_4$ with $x = 0, 0.3, 0.5, 0.7$ and 1) nanopowders were synthesized by chemical coprecipitation method. The synthesized magnetic nanoparticles were investigated by various characterization techniques, such as X-ray diffraction (XRD), vibrating sample magnetometry (VSM), scanning electron microscopy (SEM) and thermogravimetric and differential thermal analysis (TG/DTA). The XRD results confirmed the presence of cubic spinel structure of the prepared powders and the average crystallite size of magnetic particles ranging from 23 to 45 nm. The VSM results showed that the magnetic properties varied with an increase in substituted manganese while SEM analysis showed the change in the morphology of obtained magnetic nanoparticles. The TG/DTA analysis indicated the formation of crystalline structure of the synthesized samples. The heat transfer rate was measured in specially prepared magnetic nanofluids (nanoparticles dispersed in carrier fluid transformer oil) as a function of time and temperature in presence of external magnetic fields. The experimental analysis indicated enhanced heat transfer rate of the magnetic nanofluids which depended upon the strength of external magnetic field and chemical composition.

Keywords: *magnetic nanoparticles; coprecipitation; magnetic fluids; rate of heat transfer; carrier fluid*

© Wrocław University of Technology.

1. Introduction

Nanomaterials have been produced and used by humans since time immemorial. The existence of beautiful ruby red color in some ancient glass paintings and the luster deposited on some medieval pottery contain metallic spherical nanoparticles dispersed in complex way. The techniques of synthesis and deposition were a closely guarded secret and have not been completely understood even now. The modernized microscopic analysis paved way to identification and characterization of nanomaterials and the correlation of their peculiar behavior with their structure [1]. Ferrofluids are the fluids possessing magnetic nanoparticles dispersed in various non-polar or polar liquid media which have been coated by various surfactants,

such as oleic acid, dodecylamine, sodium carboxymethyl cellulose. These surfactants have been used to improve the stability and to prevent the agglomeration of the particles [2]. Heat transfer is one of important properties of ferrofluids which plays a vital role in various fields, such as aerospace, mechanical engineering, bio-engineering, pressure sensors, loud speaker coolants and smart cooling devices [3]. In metal and metal oxide nanoparticles dispersed in carrier fluids, the heat transfer rate is high as compared to conventional fluids, such as water, vacuum pump fluid, engine oil and ethylene glycol [4]. The heat transfer rate in nanofluids is dramatically increased due to the application of external magnetic field because of the effective heat conduction through the chain like structures of magnetic nanoparticles [5]. Nkurikiyimfura et al. [6] reported in his review paper about the use of magnetic nanofluids in heat transfer medium

*E-mail: mmargabandhu@yahoo.co.in

in detail by controlling parameters such as particle size distribution, particle coating, particle clustering, cluster morphology, particles flow, particle orientation and the influence of external magnetic field on heat transfer rate. Hong *et al.* [7] showed that different volume fractions of iron nanoparticles in ethylene glycol were responsible for the determination of thermal conductivity in nanofluids. Shima *et al.* [8] conducted a series of experiments and confirmed that the excellent heat transfer rate of magnetically polarizable nanofluid was due to the efficient heat transport through percolating nanoparticle paths. Further, these experiments showed that the maximum progress in heat transfer rate of ferrofluids was caused by the non-agglomerated nanoparticles dispersed in the ferrofluids. The heat transfer rate in ferrofluids can be tuned from low to high value by varying the application of external magnetic field and its applied direction [9]. For the last two decades, magnetic nanoparticles and ferrofluids have been studied as the most fascinating topics in heat transport phenomena and in different applications. The present work was carried out on synthesis and investigation of manganese substituted CoFe_2O_4 nanoparticles dispersed in carrier fluid transformer oil, subjected to external magnetic fields.

2. Experimental

2.1. Materials

The chemicals used for the preparation of magnetic nanoparticles and ferrofluids were transformer oil, sodium hydroxide pellets (NaOH), cobalt chloride ($\text{CoCl}_2 \cdot 6\text{H}_2\text{O}$), manganese chloride ($\text{MnCl}_2 \cdot 4\text{H}_2\text{O}$) and ferric chloride ($\text{FeCl}_3 \cdot 6\text{H}_2\text{O}$). They were of very high purity (99 %) and were obtained from Merck and Nice chemicals. Hence, further purification process was not necessary.

2.2. Synthesis

2.2.1. Magnetic nanoparticles

Manganese substituted cobalt ferrite nanoparticles of different compositions ($\text{Co}_{1-x}\text{Mn}_x\text{Fe}_2\text{O}_4$ with $x = 0, 0.3, 0.5, 0.7$ and 1) were synthesized by coprecipitation technique. Aqueous

solutions of chemicals $\text{CoCl}_2 \cdot 6\text{H}_2\text{O}$, $\text{MnCl}_2 \cdot 4\text{H}_2\text{O}$, $\text{FeCl}_3 \cdot 6\text{H}_2\text{O}$, each of 100 mL, were mixed in a boiling solution of NaOH (1000 mL) at 65 °C. The salt solutions in 1:2 molar ratios were added to the boiling NaOH (0.5 M) solution. The mixed solution was subjected to magnetic stirring for one hour under a constant temperature of 100 °C. The stirring time (1 h) at a constant temperature (100 °C) was high enough for the transformation of hydroxides into spinel ferrites. At the end, an appropriate amount of oleic acid was added to the boiling solution and this solution was subjected to stirring process for another one hour. The time duration was sufficient for preparation of coated manganese substituted cobalt ferrite nanoparticles. The residual solution was undisturbed for four hours to obtain precipitate. Then, the obtained precipitate was washed several times with deionized water. Further the product was washed with acetone to remove impurities and dried at room temperature [10, 11].

2.2.2. Preparation of ferrofluids

Manganese substituted cobalt ferrofluids were prepared by dispersing 4.5 g of coated manganese substituted cobalt ferrite ($\text{Co}_{1-x}\text{Mn}_x\text{Fe}_2\text{O}_4$ with $x = 0, 0.3, 0.5, 0.7$ and 1) nanopowders in 350 mL carrier fluid transformer oil. The homogenous stable solution was obtained by stirring the nanoparticles in the transformer oil at a constant speed for one hour. The coating of nanoparticles in the prepared ferrofluids prevented agglomeration of the particles caused by magnetic and van der Waals attraction forces. In addition, it provided strong electrostatic interparticle repulsion between the magnetic nanoparticles [10, 11]. Thus, the prepared Co–Mn ferrofluids were chemically stable.

2.3. Heat transfer rate analysis

The experimental arrangement for the investigation of heat transfer rate of manganese substituted cobalt ferrofluids ($\text{Co}_{1-x}\text{Mn}_x\text{Fe}_2\text{O}_4$ with $x = 0, 0.3, 0.5, 0.7$ and 1) in external magnetic fields is shown in Fig. 1. The experimental setup was constructed using an electromagnet, heater, thermometer and ferrofluid filled glass beakers. The electromagnet was designed so as to be able to accommodate with in 500 mL glass beakers.

The electromagnet was connected to an AC power supply of 230 V (50 Hz) through a rheostat to obtain variable current. Prepared ferrofluids of 350 mL volume fraction were used for heat transfer rate analysis. The heater was connected to an AC power supply of 230 V (50 Hz) and kept immersed in the ferrofluid beakers for heating process. A thermometer kept inside the fluid beaker was used to estimate the heat transfer rate as a function of time. The electromagnet was used to produce external magnetic field. In this experimental procedure, the prepared ferrofluids of different molar ratios were heated inside the ferrofluid beakers with an applied external magnetic field generated by the electromagnet through the current flow of $I = 1.8$ A and 2.7 A. The heat transfer rates per temperature of ferrofluid were recorded and analyzed.

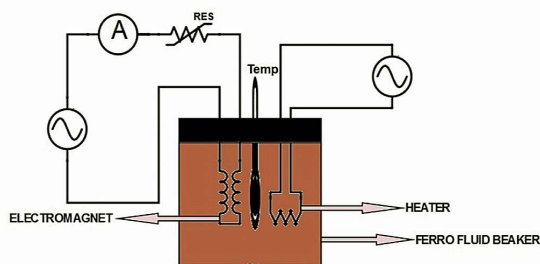


Fig. 1. Schematic setup for the investigation of heat transfer rate of Co–Mn ferrofluids in external magnetic field.

3. Characterization

3.1. X-ray diffraction

X-ray diffraction (XRD) analysis of the synthesized powder samples was carried out at room temperature by using XPERT PRO X-ray powder diffractometer with $\text{CuK}\alpha$ ($\lambda = 1.54060$ Å) radiation. The step size of 0.05° in 2θ range and scan step time of 10 s were applied in the XRD measurements. Debye-Scherrer formula was used to calculate the average crystallite size of the synthesized samples [12]:

$$D_{Xrd} = \frac{0.89\lambda}{\beta \cos \theta} \quad (1)$$

λ represents wavelength of X-ray in Å, β is full width half maximum (FWHM in radians in the 2θ scale), θ represents the Bragg's diffraction angle, D_{XRD} is crystallite size in nm.

3.2. Vibrating sample magnetometer

Hysteresis curves were obtained for the powder samples using vibrating sample magnetometer (VSM) at room temperature (Model: Lakeshore 7404) with an applied magnetic field of 20000 G. Magnetic parameters, such as coercivity (H_c), remanent magnetization (M_r) and saturation magnetization (M_s) were found from the obtained measurements.

3.3. SEM studies

Scanning electron microscope (SEM) observations were made to visualize the morphology, homogeneity and composition of the prepared magnetic nanoparticles. The differences in size obtained by the XRD analysis and SEM studies were compared and analyzed.

3.4. TG/DTA analysis

Thermogravimetric (TG) and differential thermal analysis (DTA) were made using the instrument NETZSCH STA 449F3 in air atmosphere at a heating rate of 10°C per minute.

4. Results and discussion

4.1. XRD characterization

The X-ray diffraction (XRD) patterns of manganese substituted cobalt ferrite ($\text{Co}_{1-x}\text{Mn}_x\text{Fe}_2\text{O}_4$ with $x = 0, 0.3, 0.5, 0.7$ and 1) nanoparticles are shown in Fig. 2. The diffraction peak of the reflection plane (3 1 1) of maximum intensity shows that the material has a single face centred cubic spinel phase. The reflection planes (2 2 0) (3 1 1) (5 1 1) (4 4 0) of corresponding diffraction angles 30.26° , 35.5° , 56.9° , 62.5° show that all the samples have a cubic spinel structure [13]. The peak shift for the plane (3 1 1) is caused by the lattice constant variation with manganese substitution. The lattice constant (a_0) was calculated from the obtained 'd' value with the respective (h k l) parameters.

Table 1. Summary of lattice constant values [Å] for $\text{Co}_{1-x}\text{Mn}_x\text{Fe}_2\text{O}_4$ with x varying from 0.0, 0.3, 0.5, 0.7 and 1.0.

No.	Sample	Lattice constant [Å]
1	CoFe_2O_4	8.397
2	$\text{Co}_{0.7}\text{Mn}_{0.3}\text{Fe}_2\text{O}_4$	8.424
3	$\text{Co}_{0.5}\text{Mn}_{0.5}\text{Fe}_2\text{O}_4$	8.421
4	$\text{Co}_{0.3}\text{Mn}_{0.7}\text{Fe}_2\text{O}_4$	8.466
5	MnFe_2O_4	8.493

The linear variation of lattice constant ' a_0 ' with respect to manganese content is shown in Table 1. It varies from 8.39 Å to 8.49 Å. The lattice constant values of 8.39 Å for CoFe_2O_4 and 8.49 Å for MnFe_2O_4 closely match with the proposed results [14]. The obtained results show that the increased lattice constant with an increase of manganese content in cobalt ferrite nanoparticles results from the occupying nature of Mn^{2+} ions whose atomic radius (0.83 Å) is greater than the atomic radius of Co^{2+} ions (0.78 Å) [13]. The average crystalline structure was calculated using Debye Scherrer's formula and it was in the range between 23 nm to 45 nm.

4.2. Magnetic measurements

Magnetic properties of manganese substituted cobalt ferrite nanoparticles were studied by vibrating sample magnetometer (VSM) analysis. The obtained VSM results for different compositions ($\text{Co}_{1-x}\text{Mn}_x\text{Fe}_2\text{O}_4$ with $x = 0, 0.3, 0.5, 0.7$ and 1) of magnetic nanoparticles are shown in Fig. 3. It was found that the coercivity (H_c), remanent magnetization (M_r) and saturation magnetization (M_s) vary for different molar ratios of manganese in the cobalt ferrite nanoparticles. It was observed that the coercivity (H_c) and remanent magnetization (M_r) decrease with an increase in molar ratio of manganese in cobalt ferrite nanoparticles. The saturation magnetization (M_s) starts increasing and decreasing with manganese substitution. The above trend in saturation magnetization (M_s) parameter was due to super exchange interaction mechanism between lattice positions of metal ions A and B in ferrites [15]. From the obtained results, it was

deduced that the substituted Mn^{2+} ions occupy A and B lattice positions, which results in the reduction of interaction between A and B sites. The substitution of nonmagnetic ion such as manganese, which has a preferential A site occupancy, results in the reduction of the exchange interaction between A and B sites. Hence, by varying the amount of manganese substitution, it should be possible to vary magnetic properties of the samples. In our study, the preferential occupancy of added manganese (Mn^{2+}) reduced the exchange interaction between A and B sites due to which the saturation magnetization decreased [16].

4.3. SEM analysis

Fig. 4 shows the scanning electron microscope (SEM) images of manganese substituted cobalt ferrite nanoparticles synthesized by coprecipitation method. The reported size of the nanoparticles was in between 88 nm to 71 nm which was in close agreement with the general statement that the average grain size of nanocrystalline materials is of the order of 1 to 100 nm. It was found that the grains were connected to each other all over the sample.

4.4. TG/DTA analysis

Thermogravimetric (TG) and differential thermal analysis (DTA) graphs are shown in Fig. 5. The TG/DTA analysis was made for the synthesized three powder samples with the compositions CoFe_2O_4 , $\text{Co}_{0.7}\text{Mn}_{0.3}\text{Fe}_2\text{O}_4$ and $\text{Co}_{0.5}\text{Mn}_{0.5}\text{Fe}_2\text{O}_4$. The DTA curves show the sharp endothermic peak at 110 °C which may be due to complete removal of moisture and initiation of crystalline structure of the samples. In the TGA curves, the decrement in weight percentage at 100 °C is due to water loss in the samples. The weight loss for CoFe_2O_4 is larger than for $\text{Co}_{0.7}\text{Mn}_{0.3}\text{Fe}_2\text{O}_4$ and $\text{Co}_{0.5}\text{Mn}_{0.5}\text{Fe}_2\text{O}_4$. Also CoFe_2O_4 shows slow crystallization process from 375 °C to 800 °C. The results show that manganese substitution decreased the weight loss during the crystallization process. The weight loss between 375 °C to 400 °C may be due to the decomposition of impurities present in the samples. The gradual

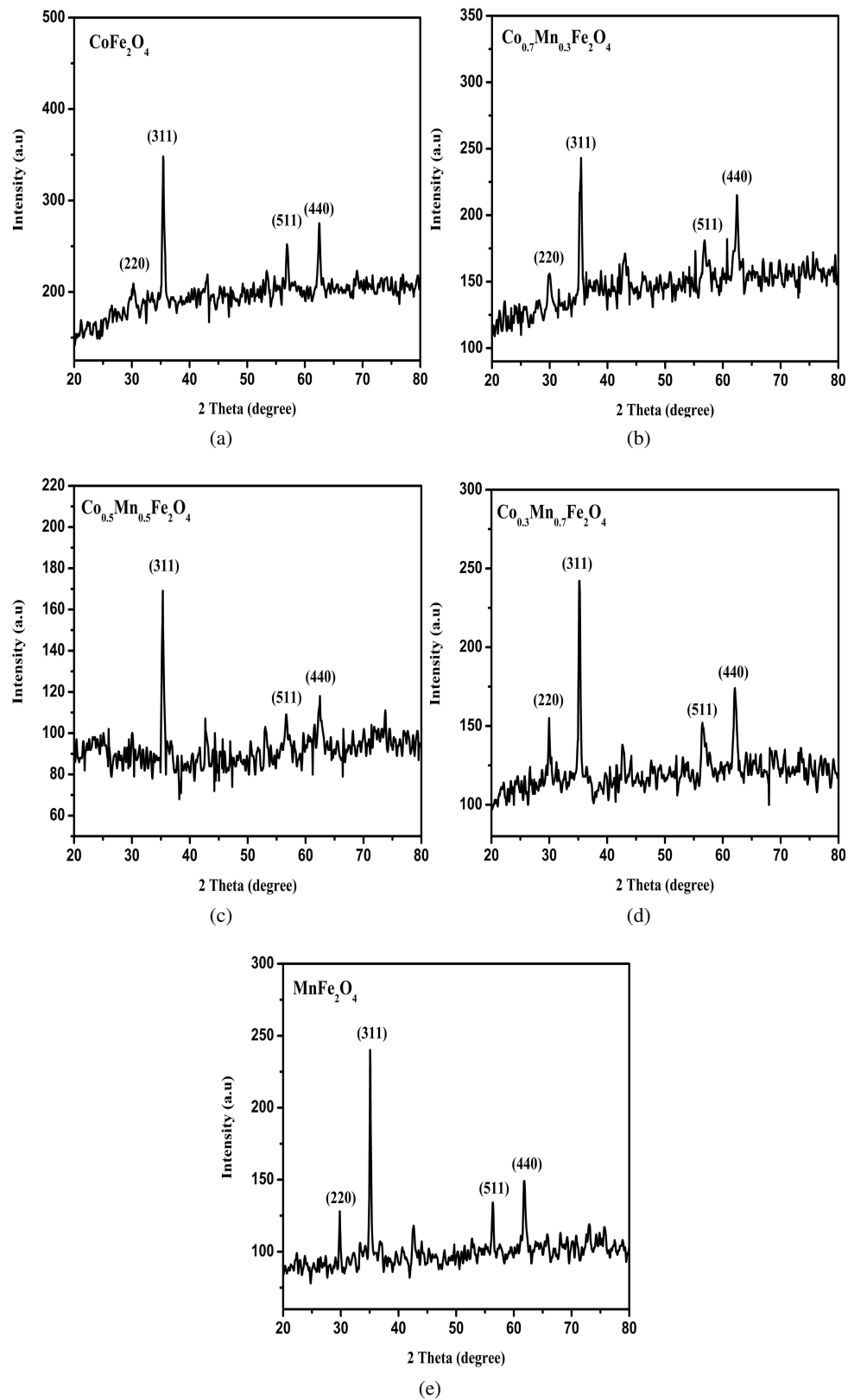


Fig. 2. Indexed X-ray diffraction patterns of (a) CoFe_2O_4 , (b) $\text{Co}_{0.7}\text{Mn}_{0.3}\text{Fe}_2\text{O}_4$, (c) $\text{Co}_{0.5}\text{Mn}_{0.5}\text{Fe}_2\text{O}_4$, (d) $\text{Co}_{0.3}\text{Mn}_{0.7}\text{Fe}_2\text{O}_4$ and (e) MnFe_2O_4 .

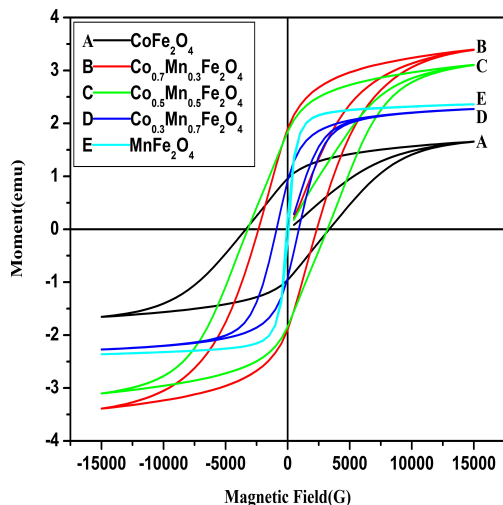


Fig. 3. Magnetization curves of CoFe_2O_4 , $\text{Co}_{0.7}\text{Mn}_{0.3}\text{Fe}_2\text{O}_4$, $\text{Co}_{0.5}\text{Mn}_{0.5}\text{Fe}_2\text{O}_4$, $\text{Co}_{0.3}\text{Mn}_{0.7}\text{Fe}_2\text{O}_4$ and MnFe_2O_4 at room temperature.

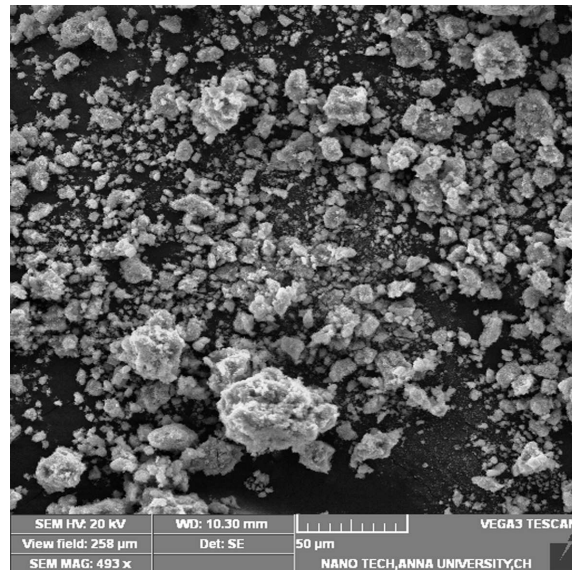
weight loss in the range of 450 °C to 800 °C was due to the formation of crystalline structure in the synthesized samples. The linear weight loss in temperature range of 500 to 800 °C confirms the complete formation of crystalline and spinel phase structure in the synthesized samples. It can be stated that the removal of adsorbed water and impurities, and formation of complete crystalline structure with spinel phase was completed at 800 °C [17, 18].

4.5. Comparative analysis on heat transfer rate of Co–Mn ferrofluids

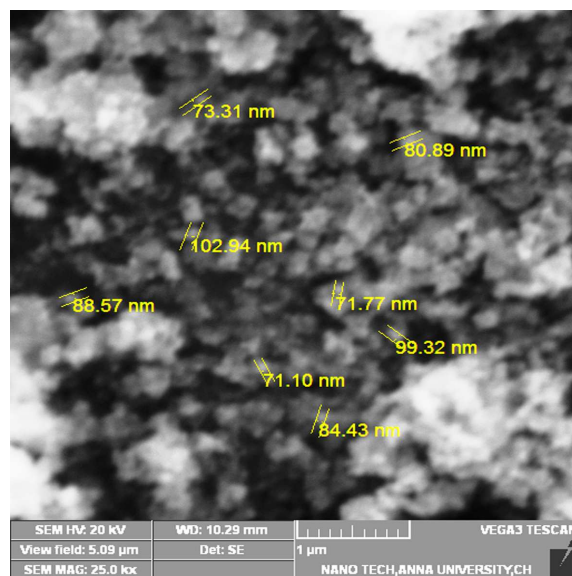
4.5.1. Aggregation of magnetic nanoparticles in magnetic field

Ferrofluids are colloidal suspensions of magnetic nanoparticles in a nonmagnetic carrier fluid possessing superparamagnetic nature and exhibiting Brownian motion whose moments are dynamic in nature. In such case, when an external magnetic field is applied, the convection velocity of nanoparticles reduces and results in chain like formation. The Brownian motion of particles almost disappears [19]:

$$v = \sqrt{18k_B T / \pi \rho d^3} \quad (2)$$



(a)



(b)

Fig. 4. SEM images of manganese substituted CoFe_2O_4 nanoparticles.

where $k_B T$ represents the thermal energy, ρ represents the density of fluid and d represents the diameter of the suspended particles. The aggregation process of the system is governed by the dipole-dipole energy between fluctuating moments given as [20, 21]:

$$U_{dd}(r) = \frac{-1}{3k_B T} \left(\frac{2m_1 m_2}{\pi \mu_0 r^3} \right) \quad (3)$$

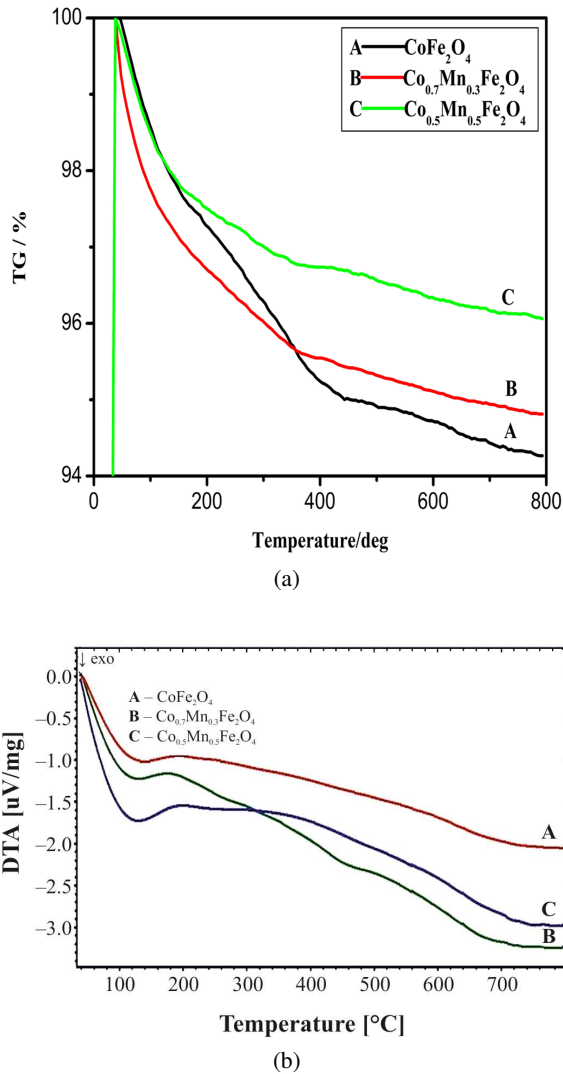


Fig. 5. (a) TG and (b) DTA results of manganese substituted CoFe₂O₄ nanoparticles with $x = 0.0, 0.3$ and 0.5 .

where U_{dd} is the dipole-dipole interaction energy and μ_0 represents permeability of free space. When an external magnetic field is applied, the dipole-dipole interaction between the moments increases, resulting in aggregation of particles in direction of the applied magnetic field. The phenomenon is similar to that of an isothermal compression of an ideal gas. The entropy of the system is defined as [21, 22]:

$$\Delta S = NK_B \ln \left(\frac{V_a}{V} \right) \quad (4)$$

where N and K_B are the number of magnetic particles and Boltzman constant.

4.5.2. Comparative analysis

An experimental analysis was carried out to investigate and compare the heat transfer rate of the ferrofluids in external magnetic fields. The experimental setup was shown in Fig. 1. Manganese substituted cobalt ferrofluid (Co_{1-x}Mn_xFe₂O₄) samples: CoFe₂O₄, Co_{0.5}Mn_{0.5}Fe₂O₄ and MnFe₂O₄ were subjected to two external magnetic field of different values. Fig. 6 shows the heat transfer rate of a CoFe₂O₄ ferrofluid at external magnetic field generated at two current values of $I = 1.8$ A and 2.7 A. The recorded average heat transfer rates per temperature in °C were 3.5 s/°C and 1.8 s/°C respectively. Fig. 7 shows the average heat transfer rates of Co_{0.5}Mn_{0.5}Fe₂O₄ ferrofluid for the above mentioned two current values which are 3.8 s/°C and 3.6 s/°C respectively. Fig. 8 shows the average heat transfer rate per temperature in °C of MnFe₂O₄ ferrofluid for the same two current values and the heat transfer rate were 3.6 s/°C and 2.1 s/°C, respectively.

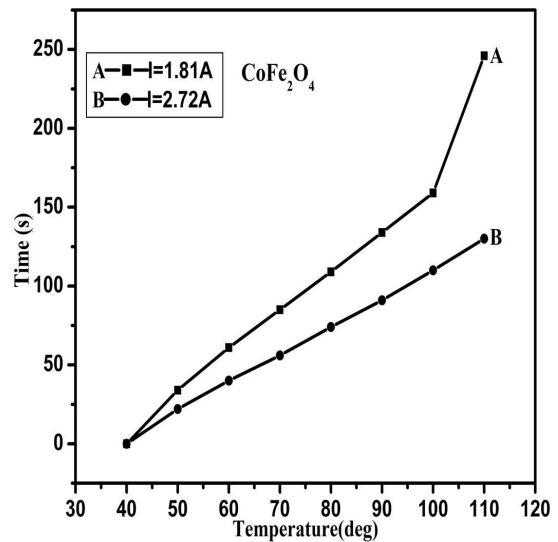


Fig. 6. Heat transfer rate of transformer oil based CoFe₂O₄ ferrofluid at an applied external magnetic fields for $I = 1.8$ A and 2.7 A.

Irrespective of the values of applied magnetic field, the heat transfer rate of single domain magnetic nanoparticle dispersed fluids (CoFe₂O₄

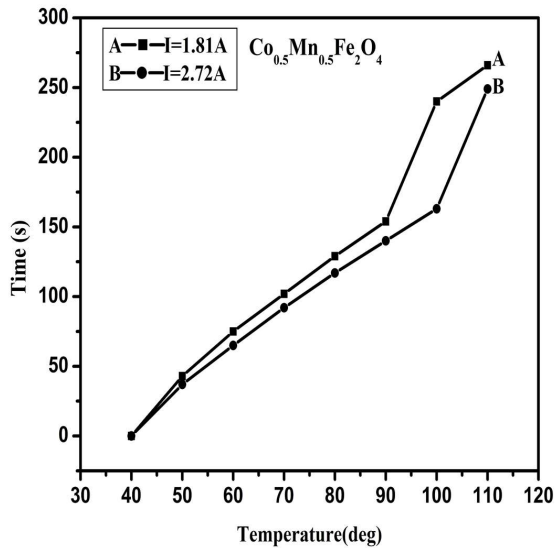


Fig. 7. Heat transfer rate of transformer oil based $\text{Co}_{0.5}\text{Mn}_{0.5}\text{Fe}_2\text{O}_4$ ferrofluid at an applied external magnetic fields for $I = 1.8$ A and 2.7 A.

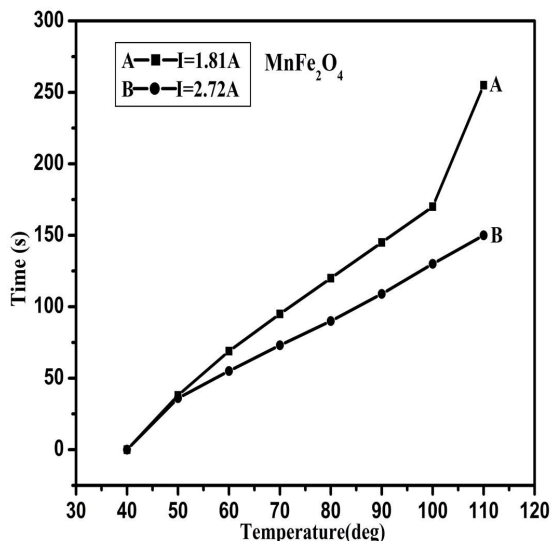


Fig. 8. Heat transfer rate of transformer oil based MnFe_2O_4 ferrofluid at an applied external magnetic fields for $I = 1.8$ A and 2.7 A.

and MnFe_2O_4) was found to be greater than that of polydispersed fluids ($\text{Co}_{0.5}\text{Mn}_{0.5}\text{Fe}_2\text{O}_4$). In both single domain and polydispersed magnetic nanoparticle dispersed fluids, the strength of the applied alternating magnetic field plays an important role in the heat transfer rate. The heat transfer rate for $I = 1.8$ A did not exhibit significant

variation among the three samples. Nkurikiyimfura *et al.* [6] found that the thermal conductivity of polydispersed magnetic nanoparticle dispersed fluid was lower than that of single domain magnetic nanoparticle dispersed fluids. It was shown that the multi domain ferro/ferri magnetic nanoparticles dispersed ferrofluids could lead to poor stability of MNFs due to their long and irreversible chain-like structures.

The heat transfer rate analysis results of manganese substituted cobalt ferrofluids ($\text{Co}_{1-x}\text{Mn}_x\text{Fe}_2\text{O}_4$ with $x = 0.0, 0.5,$ and 1) of different molar ratios were similar to the results reported by Wang *et al.* [4]. He proposed that the mixture of magnetic and non-magnetic nanoparticle dispersed carrier fluid promotes thermal conductivity.

The heat transfer rates of CoFe_2O_4 , MnFe_2O_4 and $\text{Co}_{0.5}\text{Mn}_{0.5}\text{Fe}_2\text{O}_4$ were greater for $I = 2.7$ A than for $I = 1.8$ A. The result indicates that the heat transfer rate strongly depends upon the strength of the applied external magnetic field. Similar results have been reported by Shima *et al.* [8] and Lian *et al.* [23]. They showed that the enhancement of thermal conductivity can be observed in magnetic nanofluids with increasing strength of applied alternating magnetic field in its parallel direction to the temperature gradient.

The heat transfer rate of polydispersed magnetic nanofluid $\text{Co}_{0.5}\text{Mn}_{0.5}\text{Fe}_2\text{O}_4$ was lesser than the heat transfer rate of single domain magnetic nanoparticle dispersed fluids CoFe_2O_4 and MnFe_2O_4 for both applied alternating magnetic field values: $I = 1.8$ A and $I = 2.7$ A. This result was in coincidence with the proposed result of Nkurikiyimfura *et al.* [6].

4.6. Applications

Lian *et al.* reported that synthesized magnetic nanofluids were used in automatic energy transport cooling devices in which thermal conductivity enhancement occurred along with removal of heat, when such devices were immersed in magnetic nanofluids [23]. It was also reported that the MNF layer of 10 mm thickness absorbed completely solar radiation and acted as a good heat

transfer medium in solar panel constructions [24]. This research suggests that the single domain magnetic nanoparticle dispersed fluids CoFe_2O_4 and MnFe_2O_4 could be used in heat transport phenomena. They can be more suitable for electrical devices, such as transformers, smart cooling devices and automatic energy transport systems due to their high heat transfer rate as compared to poly dispersed magnetic nanofluid sample $\text{Co}_{0.5}\text{Mn}_{0.5}\text{Fe}_2\text{O}_4$. Magnetic nanofluids may give promising results of enhanced heat transfer rate in smart cooling and thermal conduction devices as compared to conventional fluid based devices.

5. Conclusions

Manganese substituted cobalt ferrite ($\text{Co}_{1-x}\text{Mn}_x\text{Fe}_2\text{O}_4$ with $x = 0.0, 0.3, 0.5, 0.7$ and 1) nanoparticles were successfully synthesized using chemical coprecipitation method. The structural, magnetic, morphological and thermal properties of the prepared samples were analyzed using XRD, VSM, SEM and TG/DTA. XRD results confirmed that all the prepared magnetic nanoparticle powder samples had a cubic spinel structure. TG/DTA analysis showed the removal of adsorbed water, impurities and formation of complete crystalline structure of the samples with spinel phase. From VSM analysis, it was concluded that the coercivity (H_c) and remanent magnetization (M_r) decrease with an increase in molar ratio of manganese substituted cobalt ferrite nanoparticles. Homogeneous magnetic nanofluids with manganese substituted cobalt ferrite nanoparticles of different molar ratios dispersed in transformer oil were prepared. The heat transfer analysis was carried out in the prepared magnetic nanofluids in external magnetic fields. The obtained results showed that the single domain magnetic nanoparticles dispersed fluids (CoFe_2O_4 and MnFe_2O_4) exhibited enhanced heat transfer rate in comparison to poly dispersed magnetic nanofluid ($\text{Co}_{0.5}\text{Mn}_{0.5}\text{Fe}_2\text{O}_4$) for the two different applied external magnetic fields. The rate of heat transfer depended upon the strength of the applied external magnetic field. It was concluded that the manganese substituted cobalt ferrofluids ($\text{Co}_{1-x}\text{Mn}_x\text{Fe}_2\text{O}_4$) of different molar ratios can be

utilized in energy conversion devices, transformers, smart cooling devices, and in automatic energy transport devices.

Acknowledgements

One of the author. S. Sendhilnathan, gratefully acknowledges the DST (Ref. No. SERC No. 100/IFD/7194/2010-11 dated on 12.10.10) for the financial assistance received through the project.

References

- [1] MURTY B.S., *The Big World of Nanomaterials*, in: MURTY B.S., SHANKAR P., RAJ B., RATH B.B., MURDAY J., *Textbook of Nanoscience and Nanotechnology*, Springer Berlin Heiderberg, India, 2013, p. 1.
- [2] SHARIFI I., SHOKROLLAHI H., AMIRI S., *J. Magn. Magn. Mater.*, 6 (2012), 903.
- [3] ABARESHI M., GOHARSHADI E.K., ZEBARJAD S.M., FADAFAN H.K., YOUSSEFI A., *J. Magn. Magn. Mater.*, 24 (2010), 3895.
- [4] WANG X., XU X., CHOI S.U.S., *J. Thermophys Heat Transfer*, 4 (1999), 474.
- [5] PHILIP J., SHIMA P.D., RAJ B., *Appl. Phys. Lett.*, 20 (2007), 203108-1.
- [6] NKURIKIYIMFURA I., WANG Y., PAN Z., *Renew. Sust. Energy. Rev.*, 21 (2013), 548.
- [7] HONG T.K., YANG H.S., CHOI C.J., *J. Appl. Phys.*, 6 (2005), 064311-1.
- [8] SHIMA P.D., PHILIP J., *J. Phys. Chem. C.*, 41 (2011), 20097.
- [9] PHILIP J., SHIMA P.D., RAJ B., *Nanotechnology*, 30 (2008), 305706.
- [10] VAIDYANATHAN G., SENDHILNATHAN S., ARULMURUGAN R., *J. Magn. Magn. Mater.*, 2 (2007), 293.
- [11] VAIDYANATHAN G., SENDHILNATHAN S., *J. Magn. Magn. Mater.*, 6 (2008), 803.
- [12] JENKINS R., SNYDER R.L., *Introduction to X-ray Powder Diffractometry*, John Wiley & Sons Inc, New York, 1996.
- [13] ATIF M., TURTELLI R.S., GROSSINGER R., SIDDIQUE M., NADEEM M., *Ceram. Int.*, 1 (2014), 471.
- [14] PEREIRA C., PEREIRA A.M., FERNANDES C., ROCHA M., MENDES R., GARCÍA M.P.F., GUEDES A., TAVARES P.B., GRENECHE J.M., ARAUJO J.P., FREIRE C., *Chem. Mater.*, 8 (2012), 1496.
- [15] YADAV S.P., SHINDE S.S., BHATT P., MEENA S.S., RAJPURE K.Y., *J. Alloy. Compd.*, 646 (2015), 550.
- [16] SAAFAN S.A., ASSAR S.T., MANSOUR S.F., *J. Alloy. Compd.*, 542 (2012), 192.
- [17] SANPO N., BERNDT C.C., WEN C., WANG J., *Acta Biomater.*, 3 (2013), 5830.
- [18] HASHIM M., ALIMUDDIN, SHIRSATH S.E., KUMAR S., KUMAR R., ROY A.S., SHAH J., KOTNALA R.K., *J. Alloy. Compd.*, 549 (2013), 348.
- [19] PHILIP J., SHIMA P.D., RAJ B., *Appl. Phys. Lett.*, 4 (2008), 043108-1.

- [20] BISHOP K.J.M., WILMER C.E., SOH S., GRZYBOWSKI B.A., *Small*, 14 (2009), 1600.
- [21] NKURIKIYIMFURA I., WANG Y., PAN Z., *Exp. Therm. Fluid Sci.*, 44 (2013), 607.
- [22] LI J., HUANG Y., LIU X., LIN Y., BAI L., LI Q., *Sci. Technol. Adv. Mat.*, 6 (2007), 448.
- [23] LIAN W., XUAN Y., LI Q., *Energ. Convers. Manage.*, 1 (2009), 35.
- [24] LUMINOSU I., SABATA C.D., SABATA A.D., JURCA T., *AGIR Sci. Bull.*, 2 – 3 (2009), 66.

Received 2015-11-25

Accepted 2016-02-28